JOURNAL OF VIROLOGY, Sept. 2004, p. 10122–10132 Vol. 78, No. 18
0022-538X/04/$08.00+0 DOI: 10.1128/JVI.78.18.10122–10132.2004

Cytoplasmic Dynein Mediates Adenovirus Binding to Microtubules

Samir A. Kelkar,[1,2] K. Kevin Pfister,[3] Ronald G. Crystal,[1] and Philip L. Leopold[1]*

Department of Genetic Medicine,[1] and Graduate Program in Physiology and Biophysics and Systems Biology,[2] Weill Medical College of Cornell University, New York, New York, and Department of Cell Biology, University of Virginia School of Medicine, Charlottesville, Virginia[3]

Received 29 September 2003/Accepted 27 April 2004

During infection, adenovirus (Ad) capsids undergo microtubule-dependent retrograde transport as part of a program of vectorial transport of the viral genome to the nucleus. The microtubule-associated molecular motor, cytoplasmic dynein, has been implicated in the retrograde movement of Ad. We hypothesized that cytoplasmic dynein constituted the primary mode of association of Ad with microtubules. To evaluate this hypothesis, an Ad-microtubule binding assay was established in which microtubules were polymerized with taxol, combined with Ad in the presence or absence of microtubule-associated proteins (MAPs), and centrifuged through a glycerol cushion. The addition of purified bovine brain MAPs increased the fraction of Ad in the microtubule pellet from 17.3% ± 3.5% to 80.7% ± 3.8% ($P < 0.01$). In the absence of tubulin polymerization or in the presence of high salt, no Ad was found in the pellet. Ad binding to microtubules was not enhanced by bovine brain MAPs enriched for tau protein or by the addition of bovine serum albumin. Enhanced Ad-microtubule binding was also observed by using a fraction of MAPs purified from lung A549 epithelial cell lysate which contained cytoplasmic dynein. Ad-microtubule interaction was sensitive to the addition of ATP, a hallmark of cytoplasmic dynein-dependent microtubule interactions. Immunodepletion of cytoplasmic dynein from the A549 cell lysate abolished the MAP-enhanced Ad-microtubule binding. The interaction of Ad with both dynein and dynactin complexes was demonstrated by coimmunoprecipitation. Partially uncoated capsids isolated from cells 40 min after infection also exhibited microtubule binding. In summary, the primary mode of Ad attachment to microtubules occurs though cytoplasmic dynein-mediated binding.

A key requirement for viral infection or gene transfer by viral or nonviral vectors is the efficient transport of genetic material from the cell surface to the nucleus. The capsid of the adenovirus (Ad) is programmed to achieve vectorial transport of the Ad genome to the nucleus of a target cell by facilitating a sequential progression of protein-protein interactions between capsid proteins and cellular proteins. The initial interaction is the binding step involving the high-affinity interaction of the Ad fiber with the coxsackie-Ad receptor and the interaction of the Ad penton base with integrins (3, 6, 12, 24, 65, 77, 78). The interaction of Ad with its receptors enables Ad to undergo receptor-mediated endocytosis (74). After entering the cell, Ad lyses the endosomal membrane and escapes to the cytosol where it interacts with cytoplasmic dynein and microtubules, resulting in movement of Ad toward the nucleus (10, 31, 32, 36, 41, 60, 61). Finally, studies have indicated that there is a direct interaction between the Ad capsid and proteins in the nuclear envelope (9, 10, 66, 79).

The focus of the present study is the interaction of Ad with cytoplasmic dynein and microtubules. Electron microscopy studies showed Ad in close association with microtubules during infection (10, 41). Microtubule depolymerizing agents significantly reduce the amount of nuclear envelope-localized Ad 1 to 2 h postinfection in vitro (14, 32, 36, 41, 60). Ad undergoes rapid, long-range retrograde transport in neurons, suggesting an ability to form stable associations with organelles or molecular motors targeted toward the minus end of microtubules (2, 5, 17, 21, 22, 29, 30, 39, 42, 43, 46, 50, 53, 57, 64, 67, 71, 75, 80, 81). In vitro studies have shown that the Ad-microtubule interaction was enhanced by the presence of cytosolic proteins (10, 33, 76), and recently the molecular motor that drives the movement has been identified as cytoplasmic dynein. Live microscopy has shown that Ad translocation through the cytoplasm proceeds along a curvilinear track which recapitulates the known morphology of the microtubule cytoskeleton in living cells with an instantaneous velocity similar to that of cytoplasmic dynein-mediated mobility (1 to 2 μm/s) (31, 60). The elimination of cytoplasmic dynein function by the overexpression of dynamitin, a dynactin subunit protein, or by microinjection of anticytoplasmic dynein antibodies prevents Ad translocation to the nucleus and eliminates the characteristic saltatory dynamic motility of the labeled capsid (32, 60). While it is clear that Ad requires microtubules during infection and that Ad motility in cells requires functional cytoplasmic dynein, the supposition that cytoplasmic dynein promotes Ad binding to microtubules remains to be shown.

To test the hypothesis that cytoplasmic dynein promotes Ad binding to microtubules, an in vitro microtubule binding assay was established based on the ability of polymerized microtubules to induce pelleting of bound proteins upon centrifugation. By using preparations of purified bovine brain microtubule-associated proteins (MAPs) or MAPs isolated from lysates of A549 lung epithelial cells, the effect of MAPs and specifically cytoplasmic dynein on Ad-microtubule association was investigated. The results indicate that the Ad capsid association with polymerized microtubules is mediated primarily by MAPs, though an intrinsic low-level interaction between the

* Corresponding author. Mailing address: Weill Medical College of Cornell University, Department of Genetic Medicine, 515 E. 71st St., S-1000, New York, NY 10021. Phone: (212) 746-2258. Fax: (212) 746-8383. E-mail: geneticmedicine@med.cornell.edu.

Ad capsid and the microtubules was observed. The data show that the majority of the MAP-mediated Ad-microtubule binding is driven by microtubule-bound cytoplasmic dynein, thus providing direct evidence that molecular motors play roles in both linking Ad to the cytoskeleton in addition to driving Ad along microtubules during viral infection.

MATERIALS AND METHODS

Ad vectors. The Ad vector used in this study was AdNull, an Ad serotype 5 gene transfer vector that does not encode a transgene (23). The vector was propagated, purified, and stored at −70°C as previously described (54). Viral particle concentration was determined by the absorbance at 260 nm by using the extinction coefficient for Ad of 9.09×10^{-13} absorbance units/cm × mol (44). Covalent conjugation of the carbocyanine dye Cy3 (Amersham, Arlington Heights, Ill.) to the capsid proteins of Ad vectors was carried out as described previously (31, 45). Ad stocks were adjusted to a concentration of 10^{13} particles/ml and then mixed in a 1:9 ratio with Cy3 (previously reconstituted in 0.1 M sodium carbonate, pH 9.3, according to the manufacturer's instructions and then further diluted fivefold with sodium carbonate, pH 9.3). After 30 min, the reaction mixture was transferred to a dialysis chamber (10,000-molecular-weight cutoff) (Slide-a-Lyser; Pierce, Rockford, Ill.) and dialyzed against two changes of a mixture of 10% glycerol, 10 mM Tris-HCl (pH 7.5), 150 mM NaCl, and 10 mM $MgCl_2$ at 4°C for 16 h. The dialyzed mixture was then brought to 30% glycerol and stored at −20°C until use. The Cy3 dye concentration was determined by recording the absorbance at 552 nm and by using the extinction coefficient provided by the manufacturer. Dye-to-capsomere ratios were calculated on the basis of the surface exposure of 252 viral capsomeres per virion (69).

Visualization of Ad-bovine brain microtubule interaction. Purified fluorescein-conjugated bovine brain tubulin (100 μg; Cytoskeleton Inc., Denver, Colo.) was resuspended in PEM-G buffer (100 mM PIPES [pH 6.9], 1 mM EGTA, 1 mM $MgCl_2$, and 1 mM GTP) (Cytoskeleton Inc.), incubated (20 min at 35°C), and polymerized into fluorescein-conjugated microtubules by the addition of taxol (40 μM; Sigma Chemical Co., St. Louis, Mo.). Cy3-conjugated Ad capsids (10^9 particles) were incubated (40 min at 22°C) with polymerized fluorescein-conjugated microtubules in the absence or presence of purified bovine brain MAPS (4 μg; Cytoskeleton Inc.), placed over a cushion buffer composed of PEM (PEM-G without GTP) with 60% (vol/vol) glycerol with added taxol (40 μM) in Ultra-Clear centrifuge tubes (Beckman Instruments Inc., Palo Alto, Calif.) and centrifuged (100,000 × *g* for 40 min). The pellet was then resuspended in PEM buffer supplemented with taxol (40 μM) and placed on a coverslip, and fluorescein-conjugated microtubules and Cy3-conjugated Ad capsids were evaluated by fluorescence microscopy. Fluorescence microscopy was performed with an Olympus IX70 inverted microscope equipped with a ×60 numeric aperture 1.40 PlanApo objective lens. Images were acquired by using a Photometrix Quantix 57 cooled charge-coupled device camera with a 535 by 512, back-illuminated, UV-VIS coated chip operating at 3 MHz (Roper Instruments, Inc., Trenton, N.J.). Image analysis was performed with Metamorph imaging software (Universal Imaging, Downingtown, Pa.).

Quantitation of Ad-bovine brain microtubule interaction. Purified bovine brain tubulin (100 μg) was polymerized into microtubules as described above. Taxol-polymerized microtubules or unpolymerized tubulin was incubated (40 min at 22°C) in the absence or presence of purified bovine brain MAPs (10 μg), tau (10 μg; Cytoskeleton Inc.), or bovine serum albumin (10 μg) in the presence or absence of 500 mM NaCl. Cy3-conjugated Ad serotype 5 capsids (10^9 particles) were incubated under each reaction condition (40 min at 22°C) and centrifuged as described above. Supernatant was collected, and the pellet was resuspended in a volume of PEM equal to the volume of the supernatant. Equal volumes of supernatant and pellet were then boiled with protein sample buffer and run on a 10% sodium dodecyl sulfate polyacrylamide gel electrophoresis (SDS-PAGE) gel. Cy3 fluorophore-conjugated Ad capsid proteins were detected by using a Typhoon 8600 variable mode imager (Amersham Biosciences Co., Piscataway, N.J.). Total protein was evaluated by Coomassie blue staining (Bio-Rad, Hercules, Calif.). The Cy3 fluorophore-conjugated Ad hexon protein signal was quantitated by using Metamorph image analysis software (Universal Imaging).

Preparation of MAPs from A549 cell lysate and visualization of nucleotide-sensitive Ad-microtubule interaction. A549 epithelial carcinoma cells (CCL-185; American Type Culture Collection, Rockville, Md.) were cultured to confluence in Dulbecco's modified Eagle's medium (DMEM) supplemented with 10% fetal bovine serum, 100 units of penicillin per ml, and 100 μg of streptomycin (Life Technologies, Gaithersburg, Md.) per ml. Cells were harvested by scraping, suspended at density of 4×10^8 cells/ml in PEM buffer on ice, and lysed by sonication in a water-cooled Ultrasonic XL (Heat Systems, Farmingdale, N.Y.). Purified fluorescein-conjugated bovine brain tubulin was polymerized into microtubules as described above. Fluorescein microtubules were then placed over a 60% (vol/vol) glycerol-PEM buffer cushion containing taxol (40 μM) and centrifuged as described above. Supernatant was removed, and the pellet was resuspended in PEM containing taxol (40 μM). Polymerized fluorescein microtubules were added to A549 cell lysate plus taxol (40 μM) with no exogenous ATP, with 10 mM ATP, or with 10 mM adenosine imidotriphosphate (AMP-PNP; Sigma) (40 min at 22°C). Each reaction mixture was then placed over a glycerol cushion and centrifuged as described above. Pellets were then resuspended in PEM-G plus taxol with no exogenous ATP, 10 mM ATP, or with 10 mM AMP-PNP. Cy3-conjugated Ad serotype 5 capsids were incubated with the MAP-bound microtubules, prepared for centrifugation, and centrifuged as described above. Pellets were resuspended in PEM-G plus taxol with no exogenous ATP, with 10 mM ATP, or with 10 mM AMP-PNP, placed on coverslips, and evaluated by fluorescence microscopy.

Identification of motor proteins in A549 cell lysate-derived MAPs. The total protein content of the A549 cell lysate and taxol-derived A549 cell lysate pellets was determined (bicinchoninic acid protein assay; Pierce, Rockford, Ill.). Samples of equal total protein content were boiled with protein sample buffer and run on a 10% SDS-PAGE gel. The proteins were transferred (400 mA; 90 min) to nitrocellulose (Bio-Rad Inc.), and the nitrocellulose was incubated (30 min at 4°C) in blocking solution (phosphate-buffered saline with 5% nonfat dry milk and 0.05% Tween 20), washed three times in phosphate-buffered saline with 0.05% Tween 20 (5 min at 22°C), and incubated (8 h at 4°C) with mouse antidynein clone 74.1 (28) or antikinesin clone H2 (7) antibody in blocking solution (1:5,000 dilution of ascites fluid). Nitrocellulose was then incubated (60 min at 22°C) with horseradish peroxidase-conjugated donkey anti-mouse antibody (Jackson Immunoresearch Laboratories, West Grove, Pa.), and bands were detected by a chemiluminescence detection system (ECL; Amersham Life Science, Inc., Arlington Heights, Ill.).

Quantitation of nucleotide-sensitive Ad-A549-derived microtubule interaction. Endogenous tubulin of A549 cell lysate (200 μl; prepared as described above) was polymerized into microtubules by the addition of taxol (40 μM). Taxol-treated cell lysate was then centrifuged as described above to create a MAP-enriched microtubule pellet. To test the interaction of Ad with A549-derived microtubules, the pellet containing microtubules and MAPs from A549 cell lysate was resuspended in PEM-G (200 μl) plus taxol (40 μM). To test nucleotide sensitivity, the microtubule- and MAP-containing pellet was resuspended in PEM-G plus taxol (40 μM) with 10 mM MgATP or 10 mM AMP-PNP (Sigma). Cy3-conjugated Ad serotype 5 capsids (10^9 particles) were then incubated with the nonmodified or nucleotide-modified cell lysate-derived microtubules and MAPs, centrifuged, and analyzed by gel electrophoresis as described above.

Immunodepletion of cytoplasmic dynein from A549 cell lysate and effect on Ad-microtubule interaction. A549 epithelial cell lysate was prepared as described above. Cell lysate in PEM was incubated for 4 to 8 h at 4°C with a 1:100 dilution of the following immunodepletion antibodies: ascites fluid containing monoclonal anticytoplasmic dynein antibody 74.1 (28), monoclonal anticytoplasmic dynein antibody 70.1 (Sigma Immunochemicals, St. Louis, Mo.), or anti-κ light chain (Sigma Immunochemicals). Samples were then incubated with Protein A/G beads (1 h at 4°C) and centrifuged to clear antibody and target protein (three cycles of antibody and bead addition per sample were completed). Immunodepleted cell lysate was incubated with taxol and centrifuged as described above to create an immunodepleted MAP-enriched microtubule pellet. Ad interaction with immunodepleted A549-derived cell lysate microtubules and MAPs was tested by centrifugation and gel electrophoresis as described above.

Coimmunoprecipitation of cytoplasmic dynein, dynactin complex, and Ad capsid. A549 cell lysate was prepared as described above. Cell lysate was incubated with either protein A/G agarose beads (in preparation for immunoprecipitation with mouse antibodies) or protein L agarose beads (in preparation for immunoprecipitation with human antibodies) (Santa Cruz Biotechnology, Santa Cruz, Calif.) for 1 h at 4°C and centrifuged (three times) to preclear proteins that bound to the agarose beads nonspecifically. Cy3-conjugated Ad particles were added to the cell lysate and incubated (40 min at 22°C). For immunoprecipitation with anti-Ad antibodies, 2×10^{10} Ad particles were added. For immunoprecipitation with antidynein antibodies, 10^{11} Ad particles were added. The following immunoprecipitation antibodies were incubated for 4 to 8 h at 4°C: mouse ascites fluid containing monoclonal anticytoplasmic dynein antibody 74.1 (28), mouse ascites fluid containing anti-horseradish peroxidase antibody (Sigma Immunochemicals), human sera previously characterized to neutralize in vitro Ad infection (72), and human serum previously demonstrated to be nonneutralizing for

in vitro infection by Ad (72). Samples containing mouse antibodies were incubated with protein A/G (1 h at 4°C) and centrifuged to isolate antibody and target protein. Samples containing human sera were incubated with protein L beads (1 h at 4°C) and centrifuged to isolate antibody and target protein. Beads were then washed three times with PEM (with 10% glycerol). The presence of Cy3-conjugated Ad capsids in the samples was determined by SDS-PAGE and fluorescence scanning as described above. The presence of cytoplasmic dynein and dynamitin was determined by SDS-PAGE and immunoblotting (procedures described above) with antidynein intermediate chain monoclonal antibody 74.1 or antidynamitin monoclonal antibody 50.1 (47).

Interaction of partially uncoated Ad capsids with microtubules. A549 cells were cultured to 80% confluence as described above. Cells were washed three times with serum-free DMEM and infected with Ad (1,000 particles per cell) for 10 min at 27°C in serum-free DMEM. Cells were washed three times with DMEM with supplements (described above) and incubated for 40 min at 37°C. Ad-infected A549 cell lysate was then harvested as described above. To test the interaction of intracellular Ad capsids with A549 cell-derived microtubules, endogenous tubulin of Ad-infected A549 cell lysate was polymerized into microtubules by the addition of taxol (40 μM) and incubated for 80 min at 22°C. Microtubules were pelleted as described above, and the distributions of Ad capsid proteins in the supernatant and pellet were determined by Western analysis with anti-Ad human serum as described previously (72).

Statistics. Data are presented as the means of at least three independent determinations ± standard deviations of the means. The significance of differences among the means were determined by using the two-tailed Student's *t* test.

RESULTS

MAP-mediated Ad association with microtubules. To investigate the role of MAPs in the association of Ad with microtubules, the interaction of Cy3 fluorophore-conjugated Ad (red fluorescence) with microtubules polymerized from purified fluorescein-conjugated bovine brain tubulin (green fluorescence) was observed in the presence or absence of purified bovine brain MAPs. In vitro, fluorescein-tagged microtubules were observed in aster-like structures (Fig. 1). Few Cy3-labeled Ad capsids were found in association with the microtubule aster structure in the absence of MAPs. In contrast, a robust association of Ad capsids with microtubules was observed in the presence of MAPs.

When Cy3-labeled Ad was combined with microtubules, incubated, and then pelleted, the majority of the Ad remained in the supernatant (17.3% ± 3.5% of hexon signal pelleted with microtubules) (Fig. 2). The microtubule association of Ad appeared to involve an electrostatic interaction, as evidenced by the fact that a high concentration of NaCl (500 mM) prevented Ad association with microtubules (1.0% ± 0.2% in pellet; $P < 0.01$ compared to microtubules alone), consistent with prior reports of charge-dependent binding of proteins to microtubules (see reference 37 for a review). The inclusion of MAPs during the incubation of Ad with microtubules led to a significantly enhanced Ad-microtubule association, with the majority of the Ad capsid protein hexon signal found in the microtubule-associated pellet fraction (80.7% ± 3.8% in pellet; $P < 0.01$ compared to microtubules alone). A Coomassie blue stain of the gel revealed that high-molecular-weight MAPs (indicated by the >200-kDa band in Coomassie stain) copelleted with microtubules (indicated by the 55-kDa tubulin band in Coomassie stain). To evaluate the character of the MAP-dependent Ad-microtubule interaction, the binding assay was performed under high salt conditions (500 mM NaCl) to disrupt MAP-microtubule binding. In the presence of 500 mM NaCl, neither MAPs nor Ad capsids were able to cosediment with microtubules as nearly all of the Ad hexon signal was found in the supernatant (1.2% ± 0.3% of hexon signal in pellet), indicating that the interaction of Ad with MAPs and microtubules was ionic in nature. An equal amount of bovine serum albumin added to Cy3-labeled Ad and microtubules did not significantly alter Ad association with microtubules compared to incubation with microtubules alone (data not shown), demonstrating that enhancement of the Ad-microtubule association was a specific property of MAP and not a general effect of the presence of a carrier protein in the reaction.

To further evaluate the character of the MAP-dependent Ad-microtubule interaction, the binding assay was performed in the presence of a bovine brain tau protein, which is known to interact with microtubules (70). Tau protein added to Cy3-labeled Ad and microtubules did not significantly alter Ad association with microtubules compared to incubation with microtubules alone (13.9% ± 6% in pellet; $P > 0.1$ compared to microtubules), indicating that enhancement of the Ad-microtubule association was not a general property of microtubule binding proteins (Fig. 2). Tau copelleted with microtubules as indicated by Coomassie blue staining. The pelleting of Ad capsids with microtubules required the polymerization of tubulin into microtubules. Supporting this concept was the observation that when taxol was deleted from the mixture, tubulin dimers did not polymerize and remained in the supernatant, and Cy3-labeled Ad remained in the supernatant as well (1.2% ± 0.4% in pellet; $P < 0.01$ compared to polymerized microtubules and MAPs). When taxol was deleted from the reaction with MAP plus tubulin and centrifuged, tubulin dimers, MAPs, and Cy3-labeled Ad capsids remained in the supernatant (data not shown).

Cytoplasmic dynein-mediated Ad interaction with microtubules. The role of cytoplasmic dynein in mediating the Ad capsid interaction with microtubules was evaluated by using two experimental approaches. First, the nucleotide sensitivity of the Ad-microtubule interaction was assessed, and, second, the ability of a MAP fraction to support Ad-microtubule binding was evaluated following depletion of a cytoplasmic dynein.

The evaluation of the nucleotide sensitivity of the Ad-microtubule interaction was based on the knowledge that cytoplasmic dynein binds to microtubules in the absence of ATP but is released from microtubules in the presence of 10 mM ATP (48, 56). Since the release of cytoplasmic dynein from microtubules is a consequence of the ATPase activity of the enzyme, substitution of a nonhydrolyzable ATP analog, AMP-PNP, results in the adherence of cytoplasmic dynein to microtubules (48, 56). Since enzyme activity was required to demonstrate nucleotide sensitivity, a fresh source of cytoplasmic dynein was utilized with A549 lung epithelial cell lysate. To investigate the effect of ATP on the association of Ad with microtubules, the interaction of Cy3 fluorophore-conjugated Ad (red fluorescence) with A549 cell lysate MAP-bound fluorescein-conjugated bovine brain microtubules (green fluorescence) was evaluated in the absence of exogenous ATP or in the presence of ATP or AMP-PNP. In the absence of exogenous ATP, there was a robust association of Ad capsids with microtubule asters (Fig. 3A). However, in the presence of 10 mM ATP, a reduced amount of Ad associated with the microtubule structures (Fig. 3B). In the presence of 10 mM AMP-PNP, Ad capsids associated with microtubules with the same efficiency seen in the absence of ATP (Fig. 3C).

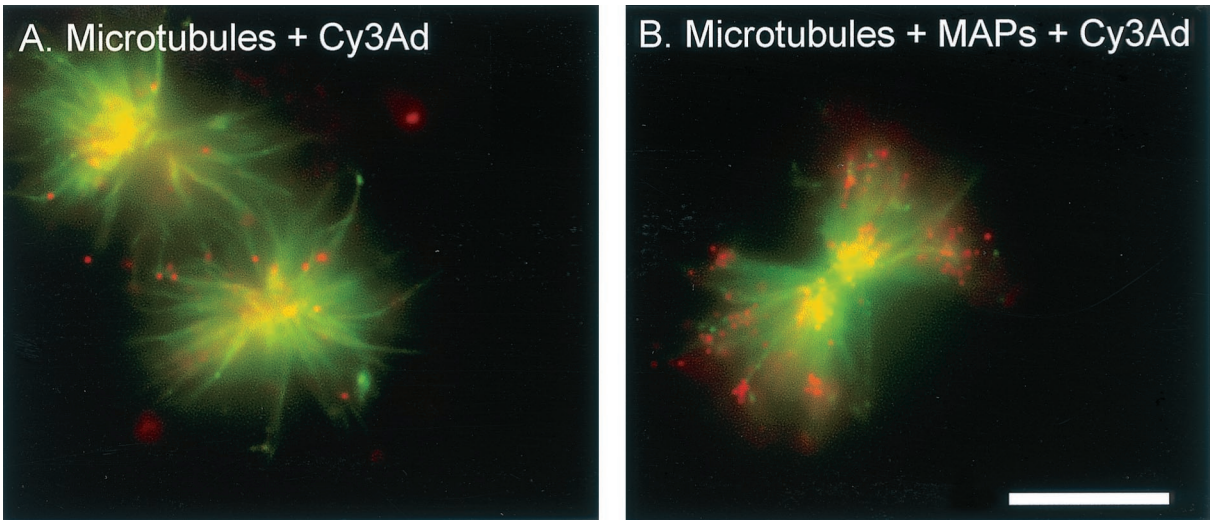

FIG. 1. Visualization of MAP-mediated Ad interaction with microtubules. Purified fluorescein-conjugated bovine brain tubulin was polymerized into microtubules by the addition of taxol. Cy3-conjugated Ad serotype 5 (Cy3Ad) capsids were incubated with microtubules in the absence or presence of purified bovine brain MAPs, pelleted, resuspended, and placed on a coverslip. Microtubules (green) and Cy3-conjugated Ad capsids (red) were evaluated by fluorescence microscopy. (A) Ad interaction with microtubules without MAPs. (B) Ad interaction with microtubules in the presence of MAPs. Bar = 5 μm.

To identify the specific molecular motors purified from A549 cell lysate in the taxol-derived pellets, samples of A549 cell lysate and resuspended taxol-derived pellets of equal total protein content were analyzed by Western analysis for the presence of dynein and kinesin (data not shown). Dynein was present in cell lysate and was 43-fold ± 4-fold more enriched in the taxol-derived pellet than in the initial cell lysate. However, kinesin was detected in the cell lysate and was not enriched in the taxol-derived pellet (data not shown). These data recapitulate previously described results which have demonstrated that a high concentration of AMP-PNP is required to purify kinesin with taxol-derived microtubules from cell lysate (8, 68, 73).

The observation that the Ad interaction with microtubules was sensitive to ATP was further explored by using a quantitative centrifugation-based assay of Ad-microtubule association. In the presence of ATP, there was a significant loss of Ad from the microtubule-associated pellet compared to Ad incubated in the absence of exogenous ATP (48.5% ± 5.6% in pellet; $P < 0.05$ compared to cell lysate alone) (Fig. 4). In the presence of 10 mM AMP-PNP, Ad bound efficiently to microtubules (83.2% ± 5.6% in pellet; $P > 0.7$ compared to cell lysate), indicating that the ATP-dependent release of Ad from microtubules required an ATPase activity. In the presence of 500 mM NaCl, Ad capsids failed to interact with microtubules in the presence of A549-derived MAPs (0.85% ± 0.32% in pellet; $P < 0.05$ compared to cell lysate alone), indicating that the interaction of Ad with cell lysate-derived MAPs and microtubules, as observed previously with bovine brain, is determined by ionic interactions. A Coomassie blue stain of the gel revealed that high-molecular-weight A549-derived MAPs (indicated by the >200-kDa band in Coomassie staining) copelleted with endogenous microtubules (indicated by the 55-kDa tubulin band in Coomassie staining) except in the presence of 500 mM NaCl. Western analysis demonstrated that dynein (indicated by the 74-kDa band in the Western analysis) recapitulated the pelleting characteristics of the Ad capsids under the various nucleotide conditions. Dynein remained bound in the pellet without the addition of exogenous ATP. In the presence of 10 mM ATP, the reduced ability of dynein to interact with microtubules led to a shift of Ad capsid toward the supernatant. In the presence of the nonhyrdolyzable analog of ATP, AMP-PNP, dynein remained in the microtubule-associated pellet fraction. In the presence of 500 mM NaCl, dynein no longer bound microtubules and was present only in the supernatant fraction.

The importance of cytoplasmic dynein in mediating the Ad capsid interaction with A549-derived microtubules was evaluated by observing the Ad-microtubule interaction in the presence of purified A549 MAPs prepared from cell lysate that had been immunodepleted of cytoplasmic dynein (Fig. 5). When Ad was mixed with microtubules and the whole MAP fraction from A549 cells, Ad pelleted in association with microtubules (84.3% ± 8.2% in pellet). In contrast, when Ad was mixed with microtubules and the A549 MAP fraction following immunodepletion of cytoplasmic dynein, Ad did not pellet efficiently with microtubules (24.8% ± 3.6% in pellet; $P < 0.01$ compared to nonimmunodepleted cell lysate). Immunodepletion of A549 MAPs with another monoclonal anticytoplasmic dynein antibody, 70.1, yielded similar results as with MAPs immunodepleted by antibody 74.1 (data not shown). Cell lysate immunodepleted with an irrelevant primary antibody (anti-κ light chain) did not demonstrate any significant alteration in the ability of the lysate to support Ad-microtubule interaction (83.2% ± 7.4% in pellet; $P > 0.9$ compared to nonimmunodepleted cell lysate alone), demonstrating that the immunodepletion protocol was not responsible for the alteration in Ad-microtubule interaction. A Coomassie blue stain of the gel revealed that high-molecular-weight A549-derived MAPs (indicated by the >200-kDa band in Coomassie staining) copel-

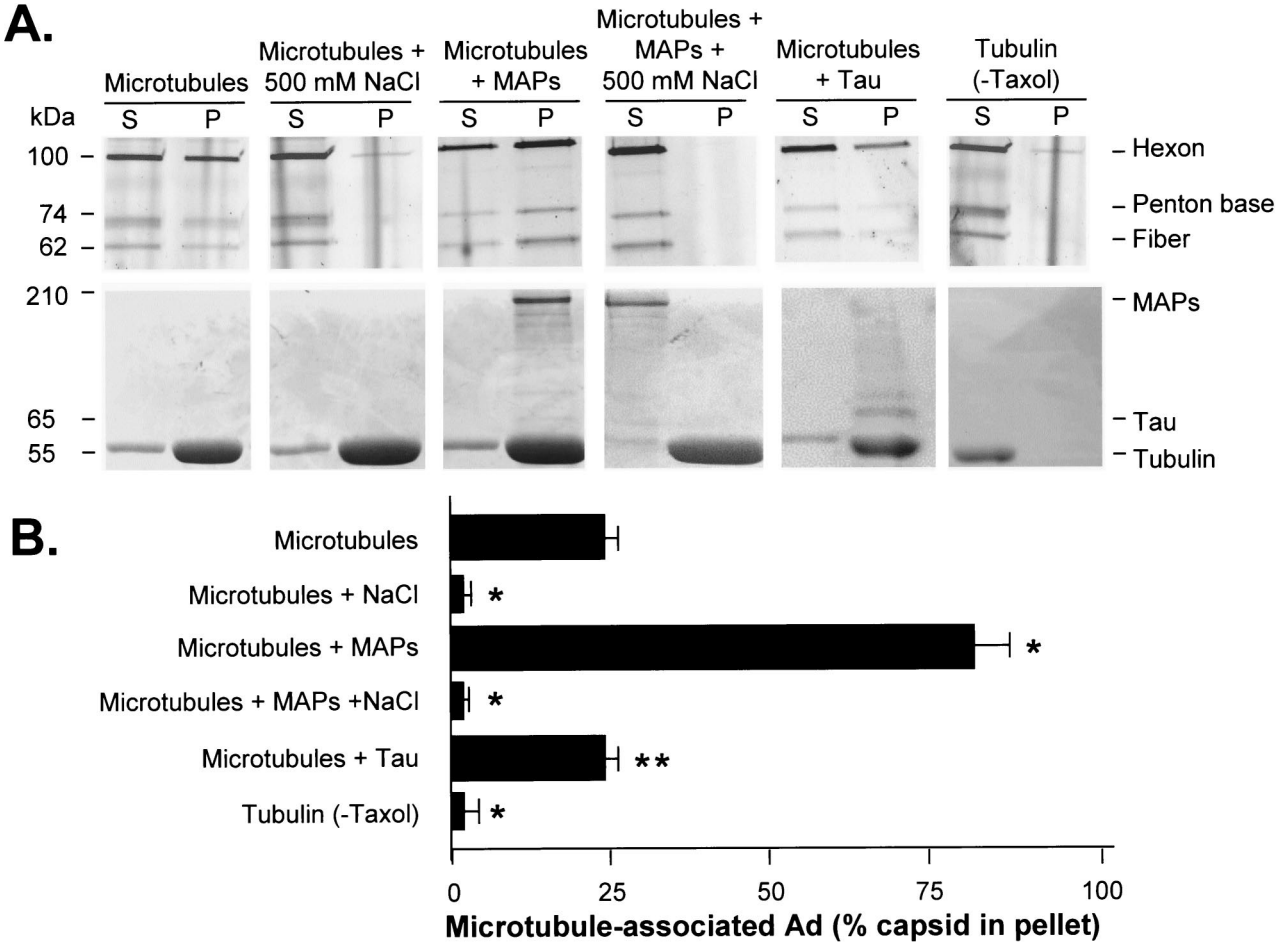

FIG. 2. Quantitative analysis of MAP-dependent Ad interaction with microtubules. Purified bovine brain tubulin dimers were polymerized into microtubules as described in the legend of Fig. 1. Taxol-polymerized microtubules or unpolymerized tubulin was incubated in the absence or presence of purified bovine brain MAPs or tau in the presence or absence of 500 mM NaCl. Cy3-conjugated Ad serotype 5 capsids were incubated under each reaction condition, placed over a glycerol cushion, and centrifuged. Supernatant (S) and pellet (P) were then analyzed by gel electrophoresis. (A) Fluorescence scan and Coomassie blue stain. Cy3-conjugated Ad capsid protein distributions in the supernatant and pellet were evaluated by fluorescence scan: hexon (106 kDa), penton base (74 kDa), and fiber (62 kDa) are shown. Tubulin and MAP distributions in the supernatant and pellet were evaluated by Coomassie blue stain: high-molecular-weight MAPs (>200 kDa), tau (65 kDa), and tubulin (55 kDa) are shown. (B) Quantitation of hexon fluorescence signal in pellet by digital analysis as a percentage of total (supernatant plus pellet) signal. Data are presented as the means and standard deviations of four separate experiments. *, significant difference compared to control ($P < 0.01$); **, no significant difference compared to control ($P > 0.1$).

leted with endogenous microtubules (indicated by the 55-kDa tubulin band in Coomassie staining) under all three treatment conditions. Western analysis demonstrated that dynein (indicated by the 74-kDa band in the Western analysis) recapitulated the pelleting characteristics of the Ad capsids under the various treatment conditions. Dynein was present in the pellet fraction under nontreated and irrelevant antibody-depleted conditions. In comparison, the total amount of dynein (supernatant plus pellet) was reduced in the dynein-depleted sample.

Interaction of Ad with cytoplasmic dynein and dynactin. The preceding data demonstrated that Ad interacted with microtubules in a cytoplasmic dynein-dependent manner, leading to the hypothesis that cytoplasmic dynein formed a link between Ad and the microtubule. A corollary of this hypothesis was that Ad and cytoplasmic dynein should interact in solution in the absence of microtubules. Furthermore, based on prior data demonstrating that overexpression of dynamitin, a dynactin complex subunit, disrupted Ad transport to the nucleus (60), there existed the possibility that the dynactin complex would also associate with Ad and cytoplasmic dynein in solution. To test these hypotheses, a mixture containing cell lysate and Ad capsids was assayed by immunoprecipitation with anticytoplasmic dynein antibodies or anti-Ad antiserum (Fig. 6). The anticytoplasmic dynein immunoprecipitate contained cytoplasmic dynein, dynamitin, and Ad capsid proteins. However, when the immunoprecipitation was carried out with an irrelevant primary antibody or when cell lysate was omitted from the experiment, no dynein, dynamitin, or Ad capsid proteins were detected in the immunoprecipitate. Conversely, the anti-Ad immunoprecipitate contained Ad capsid proteins, cytoplasmic dynein, and dynactin. In contrast, immunoprecipitates collected by using a nonimmune serum or by using anti-

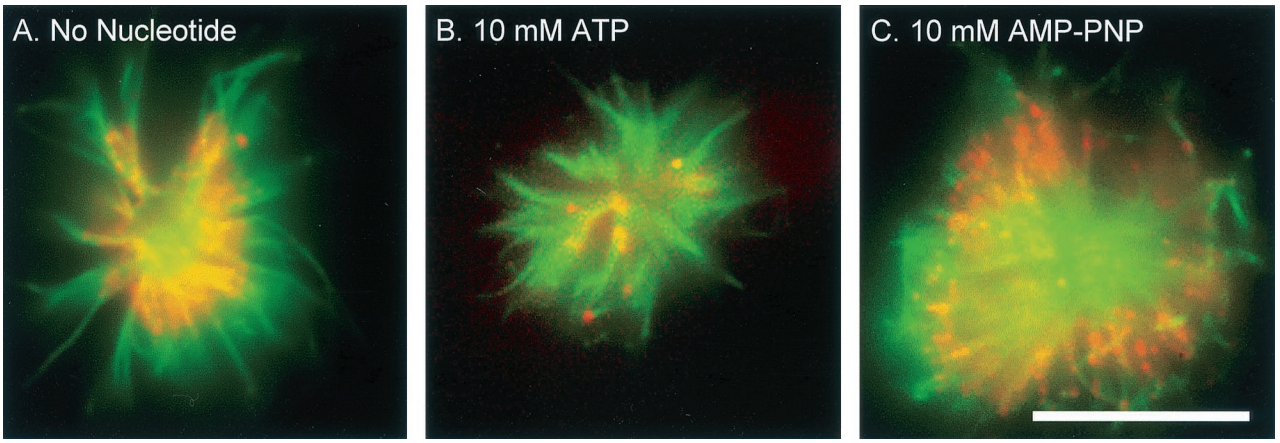

FIG. 3. Nucleotide-sensitive Ad interaction with microtubules. Purified fluorescein-conjugated bovine brain tubulin was polymerized into microtubules by the addition of taxol. Fluorescein-microtubule solution was then placed over a cushion and centrifuged, and the pellet was resuspended with taxol. A549 lung epithelial cells were harvested and lysed, and polymerized fluorescein microtubules were added to the lysate with no exogenous ATP, with ATP, or with AMP-PNP. Fluorescein-microtubule solution was then placed over a cushion and centrifuged, and the pellet was resuspended with taxol. The pellets from the reactions were resuspended, and Cy3-conjugated Ad serotype 5 capsids were incubated with the MAP-bound microtubules and assessed by fluorescence microscopy. Microtubules (green) and Cy3-conjugated Ad capsids (red) were evaluated by fluorescence microscopy. (A) Ad interaction with microtubules without exogenous nucleotide. (B) Ad interaction with microtubules in the presence of ATP. (C) Ad interaction with microtubules in the presence of AMP-PNP. Bar = 5 μm.

Ad serum without the prior addition of Ad to the cell lysate did not contain Ad capsid proteins, cytoplasmic dynein, or dynactin.

Association of partially uncoated intracellular Ad capsids with microtubules. The data presented above were collected by using a model system that employed Ad purified on a cesium chloride gradient following propagation in 293 cells. This source of virus represents extracellular virus that has not encountered the cell membrane, the endosome, or the cytosol. To test the ability of the partially uncoated, cytosolic form of

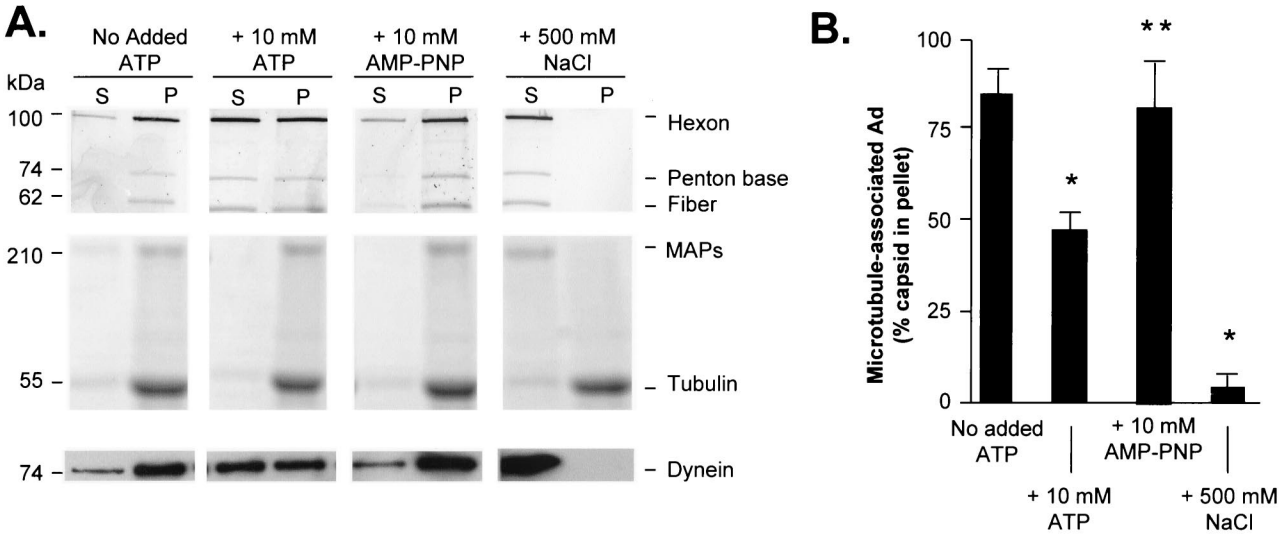

FIG. 4. Quantitative assessment of nucleotide-dependent binding of Ad with microtubules and MAPs purified from A549 cell lysate. A549 lung epithelial cell lysate was prepared as described in the legend of Fig. 3. Microtubules and MAPs from cell lysate were purified after incubation with taxol as described in Materials and Methods. Pellets containing polymerized microtubules and MAPs were resuspended in PEM-G containing no exogenous ATP, 10 mM ATP, or 10 mM AMP-PNP (a nonhydrolyzable analog of ATP). Cy3-conjugated Ad serotype 5 capsids were added to each reaction mixture, placed over a cushion buffer composed of PEM with 60% (vol/vol) glycerol, and centrifuged as described in Materials and Methods. Supernatant (S) and pellet (P) were then analyzed by gel electrophoresis and Western analysis. (A) Fluorescence scan and Coomassie blue stain. Cy3-conjugated Ad capsid protein distributions in the supernatant and pellet were evaluated by fluorescence scanning: hexon (106 kDa), penton base (74 kDa), and fiber (62 kDa) are shown. Tubulin and MAP distributions in the supernatant and pellet were evaluated by Coomassie blue staining: high-molecular-weight MAPs (>200 kDa) and tubulin (55 kDa) are shown. The presence of dynein (74 kDa) in the supernatant and pellet was evaluated by Western analysis. (B) Quantitation of hexon fluorescence signal in pellet by digital analysis as a percentage of total (supernatant plus pellet) signal. Data are presented as the means and standard deviations of four separate experiments. *, significant statistical difference compared to control ($P < 0.05$); **, no significant statistical difference compared to control ($P > 0.7$).

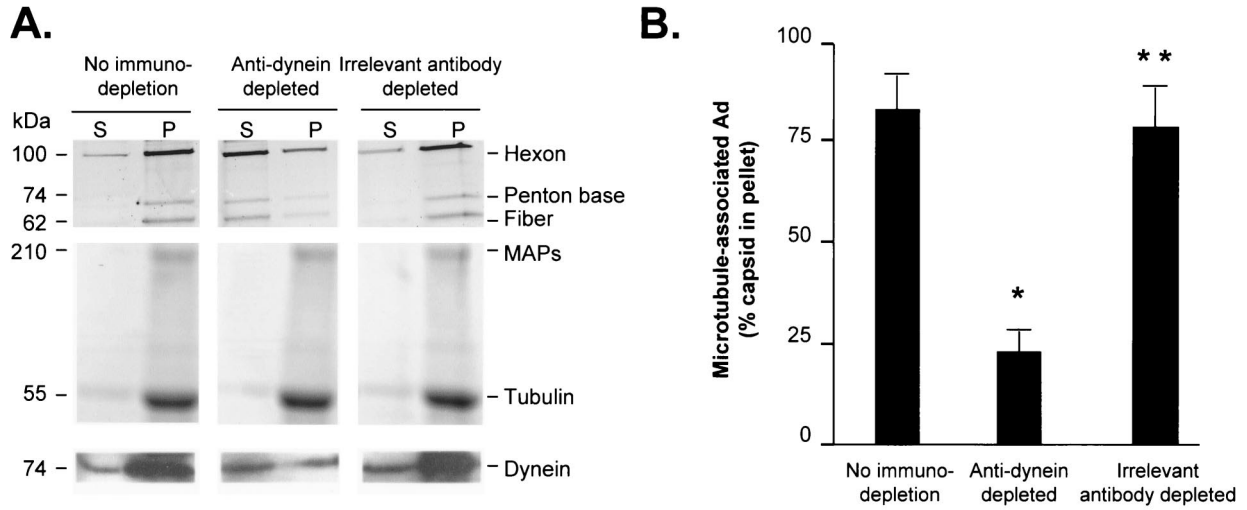

FIG. 5. Contribution of cytoplasmic dynein in MAP-enhanced Ad interaction with human cell line-derived microtubules. A549 lung epithelial cells (10 confluent 150-mm dishes) were harvested and lysed by sonication in PEM buffer on ice. Antibodies for immunodepletion of the lysate were added to cell lysate and incubated (4 to 8 h at 4°C). Immunodepletion antibodies included ascites fluid containing monoclonal anticytoplasmic dynein antibody 74.1 and anti-κ light chain. Protein A/G beads were then added to clear antibody and target protein. Endogenous tubulin was polymerized into microtubules by the addition of taxol (40 μM). Taxol-treated cell lysate was then placed over a cushion composed of PEM buffer with 60% (vol/vol) glycerol plus taxol (40 μM) and centrifuged (100,000 × *g* for 40 min). Pellets containing polymerized microtubules and MAPs were resuspended in PEM-G. Cy3-conjugated Ad serotype 5 capsids (10^9 particles) were incubated with microtubules and MAPs, placed over a cushion composed of PEM buffer with 60% (vol/vol) glycerol plus taxol (40 μM), and centrifuged (100,000 × *g* for 40 min). Supernatant (S) and pellet (P) were then analyzed by gel electrophoresis. (A) Fluorescence scan and Coomassie blue stain. Cy3-conjugated Ad capsid protein distribution in the supernatant and pellet was evaluated by a fluorescence scan: hexon (106 kDa), penton base (74 kDa), and fiber (62 kDa) are shown. Tubulin and MAP distributions in the supernatant and pellet were evaluated by Coomassie blue staining: high-molecular-weight MAPs (>200 kDa) and tubulin (55 kDa) are shown. The presence of dynein (74 kDa) in the supernatant and pellet was evaluated by Western analysis. (B) Quantitation of hexon fluorescence signal in the pellet by digital analysis as a percentage of total (supernatant plus pellet) signal. Data are presented as the means and standard deviations of four separate experiments. *, significant statistical difference compared to control ($P < 0.01$); **, no significant statistical difference compared to control ($P > 0.9$).

the virus capsid to interact with microtubules, cell lysate was prepared from A549 cells 40 min after infection with unlabeled Ad capsids. Microtubules were polymerized within the lysate and pelleted through a sucrose cushion, with analysis of Ad capsid proteins by Western analysis (Fig. 7). The Ad hexon protein, which is the principle component of the partially uncoated Ad capsid, pelleted only in the presence of intact microtubules, similar to intact virus. In contrast, the penton base and fiber proteins that release from the capsid during the initial phase of uncoating did not pellet with microtubules, demonstrating that the capsid was partially uncoated and that the main body of the capsid interacted with microtubules.

DISCUSSION

Cytoplasmic dynein has been implicated in the intracellular trafficking of Ad as well as several other viral capsids or nucleocapsids that function to deliver viral genomes to the nucleus (13, 32, 40, 51, 58, 59, 61). The involvement of cytoplasmic dynein has thus far been demonstrated through the use of function-blocking assays rather than through evidence of direct biochemical interaction. In the present study, morphological and quantitative biochemical evidence demonstrated that fractions of MAPs enhance the binding of Ad to polymerized microtubules. The binding was a property of the complete MAP fraction but was present neither in a MAP fraction specifically enriched for tau nor in MAP fractions depleted by immunoprecipitation of cytoplasmic dynein. Cytoplasmic dynein was further implicated in the binding of Ad to microtubules by the demonstration that Ad could be released from microtubules by ATP but not by AMP-PNP, a hallmark of cytoplasmic dynein-dependent microtubule binding (48, 56). Together, these data demonstrate that Ad binds to microtubules through cytoplasmic dynein, thus providing direct evidence that molecular motors play roles in both linking Ad to the cytoskeleton and in driving Ad along microtubules during viral infection.

Role of cytoplasmic motors. Microtubule-based viral motility has long been implicated in the infection pathway of viruses (11, 34). Many reports have documented the fact that Ad capsids are located adjacent to microtubules in the cell and that the inhibition of microtubule-based motility prevents viral capsids from reaching the nucleus (11, 15, 32, 36, 60, 62). Most strikingly, recent data demonstrate that the depolymerization of microtubules decreases virus-mediated gene expression at 4 h after infection, a time scale consistent with the acute inhibition of genome delivery to the nucleus (36). Thus, the phenomenon of Ad interaction with and transport along microtubules as part of the normal infection pathway is well established. Further insight into the mechanism of virus-microtubule interaction may yield important insight into the inhibition of this pathway for antiviral therapy as well as for commandeering this pathway for viral or nonviral gene transfer.

While the present studies demonstrated the importance of

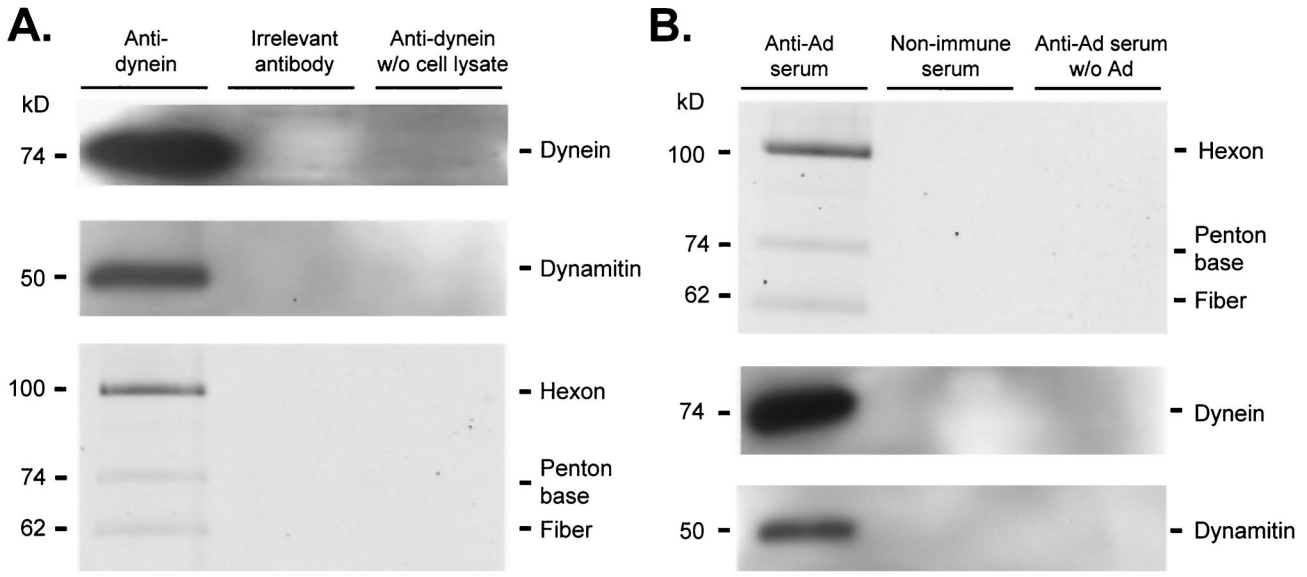

FIG. 6. Coimmunoprecipitation of cytoplasmic dynein, dynamitin, and Ad. A549 cell lysate was prepared as described in Materials and Methods. Cell lysate in PEM was incubated with either protein A/G or protein L agarose beads for 1 h at 4°C and centrifuged to preclear nonspecific agarose bead binding proteins (three times). Cy3-conjugated Ad serotype 5 capsids (2×10^{10} particles) were added to cell lysate and incubated (40 min at 22°C). Immunoprecipitation antibodies (mouse ascites fluid containing monoclonal anticytoplasmic dynein antibody 74.1, mouse ascites fluid containing anti-horseradish peroxidase antibody, human sera previously characterized to neutralize in vitro Ad infection, and human serum previously demonstrated to be nonneutralizing for in vitro infection by Ad) were incubated for 4 to 8 h at 4°C. Samples containing mouse antibodies were incubated with protein A/G (1 h at 4°C) and centrifuged to isolate antibody and target protein. Samples containing human sera were incubated with protein L beads (1 h, 4°C) and centrifuged to isolate antibody and target protein. Beads were then washed three times with PEM (with 10% glycerol). Immunoprecipitated proteins were analyzed by gel electrophoresis (A) Fluorescence scan and immunoblot of antidynein immunoprecipitated proteins. Cy3-conjugated Ad capsid protein presence was evaluated by a fluorescence scan: hexon (106 kDa), penton base (74 kDa), and fiber (62 kDa) are shown. The presence of dynein (74 kDa) and dynamitin (50 kDa) was evaluated by Western analysis. (B) Immunoblot and fluorescence scan of anti-Ad immunoprecipitated proteins. The presence of dynein (74 kDa) and dynamitin (50 kDa) was evaluated by Western analysis. Cy3-conjugated Ad capsid protein presence was evaluated by a fluorescence scan: hexon (106 kDa) penton base (74 kDa), and fiber (62 kDa) are shown.

cytoplasmic dynein in Ad binding to microtubules, the viral proteins and cytoplasmic dynein subunits involved in the interaction remain to be determined. The literature contains precedents for the direct interaction of cytoplasmic dynein with viral proteins. Recent studies have shown that specific purified recombinant subunits of the cytoplasmic dynein motor complex can bind to recombinant capsid and tegument proteins of viruses (herpes virus, rabies virus, lyssavirus, and African swine fever virus) (1, 25, 52, 82, 83). These studies have identified potential interacting elements between the recombinant cytoplasmic dynein motor complex proteins and recombinant viral capsid proteins; however, they have not definitively demonstrated that whole viral capsid binds to microtubules in a cytoplasmic dynein-dependent manner. A recent report documented the interaction between cytoplasmic dynein and intact canine parvovirus capsid, which, like Ad, is a nonenveloped virus (59). Suikkanen et al. (59) used a biochemical in vitro analysis to demonstrate direct dynein-canine parvovirus interaction.

While Ad may bind directly to cytoplasmic dynein, it is also possible that one or more accessory proteins are required to link Ad to microtubules. One obvious candidate would be the dynactin protein complex, which is known to interact with the dynein motor complex (18, 55). Overexpression of the dynactin complex member dynamitin disrupts microtubule-mediated Ad translocation (60). The observation that dynamitin coprecipitated with Ad and cytoplasmic dynein is consistent with this possibility. Another report detailed an interaction of the Ad E3-14.7K protein with the TCTEL1 subunit (mouse homolog of hTCTEX1) of cytoplasmic dynein through an intermediate cellular protein FIP-1 (35). Since Ad E3-14.7K has not been reported as a component of the Ad capsid, the significance of the interaction is likely related to the production of new viral capsids in wild-type Ad infection of cells rather than to the interaction of the Ad capsid with cytoplasmic dynein during the initial infection of a target cell.

The present study does not address the potential contribution of kinesin in Ad interaction with microtubules. Prior observations that movement of fluorophore-conjugated Ad capsid along the microtubule cytoskeleton occurred both in the direction of the nucleus as well as in the direction of the cell periphery led to the proposal that the plus-end-directed movement of the fluorophore-labeled Ad capsid might reflect a potential interaction of Ad with kinesin, a plus-end-directed molecular motor (60, 61). In the present study, studies documenting the involvement of dynein in the Ad-microtubule interaction were conducted by using a two-step procedure. In the first step, MAP-containing microtubule pellets were prepared from cell lysate. The first step did not include the addition of AMP-PNP, a condition required for the association of kinesin with microtubules (7, 68, 73). As a result, there was no enrichment of kinesin in MAPs prepared from A549 cell lysate, while

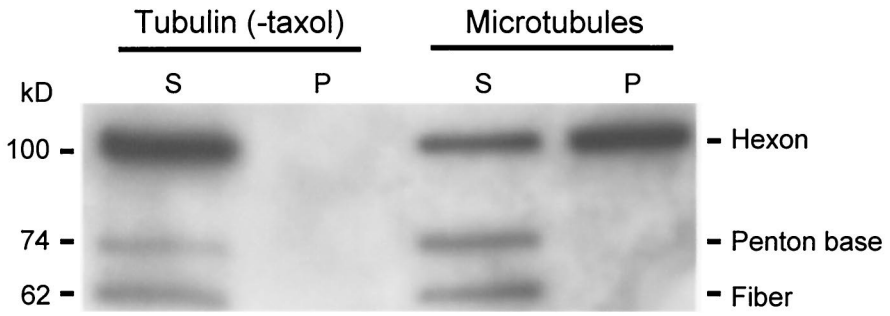

FIG. 7. Intracellular Ad particles interact with human cell line-derived microtubules in a nucleotide-sensitive manner. A549 cells were cultured to 80% confluence as described in Materials and Methods. Cells were washed three times with serum-free DMEM and infected with Ad5 (1,000 particles/cell) for 10 min at 37°C in serum-free DMEM. Cells were washed three times with serum containing DMEM and incubated for 40 min at 37°C. Ad-infected A549 cell lysate was then harvested as previously described. To test the interaction of intracellular Ad capsids with A549-derived microtubules, endogenous tubulin of Ad-infected A549 cell lysate was polymerized into microtubules by the addition of taxol (40 μM) and incubated for 80 min at 22°C. Reactions were centrifuged as described previously. The presence of Ad capsid in the supernatant (S) and pellet (P) was evaluated by SDS-PAGE and Western analysis.

cytoplasmic dynein was enriched 43-fold ± 4-fold compared to its concentration in cell lysate. During the second step, the nucleotide dependence of the Ad-microtubule interaction was characterized by the addition of either ATP or the nonhydrolyzable ATP analog AMP-PNP. The addition of AMP-PNP in the second step was designed as a control for the addition of ATP but was not relevant to the question of the Ad-kinesin interaction. Furthermore, reaction buffers used in the Ad-microtubule interaction assay contained GTP, a condition that has been demonstrated to elute kinesin from microtubules during the preparation of MAP fractions (7, 73). To assess the potential interactions of Ad with kinesin, a separate experimental protocol for the preparation of MAPs from cell lysate would be required.

The identity of the Ad capsid protein that interacts with the dynein/dynactin/microtubule complex will also require further investigation. In the present study, both intracellular uncoated capsid as well as extracellular intact capsid were shown to interact with microtubules. Therefore, the mechanism of interaction is likely to involve a viral protein that is accessible on the surface of the capsid prior to uncoating. The failure of penton base and fiber to interact with microtubules limits the possibility that these two elements are involved. The candidates include hexon, protein IX, protein VI, and perhaps the L3/p23 protease, which is accessible to modification by sulfhydryl alkylating agents (20). Among these possibilities, it is interesting that the L3/p23 protease (GenBank accession number DAA00654) contains a consensus binding site for dynein light chain that has been identified in other viral and nonviral proteins (38). At the same time, the specificity for the interaction may reside entirely with the dynein/dynactin complex which has exhibited an ability to direct the transport of other protein aggregates toward the microtubule organizing center (16, 26).

Direct Ad-microtubule interactions. In addition to the cytoplasmic dynein-dependent binding of Ad to microtubules, a secondary interaction of Ad with microtubules was observed. In the absence of MAPs, approximately 20% of the Ad signal was found in the pellet with polymerized microtubules (tubulin plus taxol) but not when centrifuged with tubulin subunits alone. This significant proportion of Ad was found in the pellet in the absence of MAPs, in the presence of the tau fraction, or in the presence of a nonspecific protein (bovine serum albumin). In contrast, no Ad was found in the microtubule pellet when the incubation was performed in the presence of 500 mM NaCl, indicating that this interaction may be comprised of electrostatic forces between Ad and microtubules. Similar interactions between cytosolic proteins and microtubules have been noted previously (37), but the physiological significance of this interaction, if any, remains to be determined. One additional possibility for the nonspecific Ad-microtubule interaction could have been a physical interaction of microtubules with Ad, comparable to viral capsid being trapped in a net. This possible explanation is unlikely, based on the observations made in the presence of tau protein. The tau protein is capable of cross-linking microtubules and, therefore, would be expected to change the character of the microtubule net. The very good agreement between the amount of Ad that pelleted in the absence of all protein compared to the amount that pelleted in the presence of tau protein argued that the mass of microtubules rather than their physical arrangement accounted for the amount of Ad that pelleted in the absence of MAPs. Interestingly, in at least two viruses (JHM coronavirus and herpes simplex virus), viral proteins contain tau-like domains that mediate the direct binding of viral capsid to microtubules (27, 49, 63). If this mechanism were operating with Ad capsid proteins, one might expect tau to compete with Ad for microtubule binding. While a formal kinetic study was not performed here, the lack of difference in Ad binding to microtubules in the presence or absence of tau suggests that molecular mimicry of tau would not explain the MAP-independent Ad-microtubule interaction.

Postmicrotubule processes. Ad, after escape from the endosome, is presented with the challenge of moving from the cell periphery to the nucleus. Ultimately, the capsid must accomplish delivery of the Ad genome to the nucleus. While interaction with cytoplasmic dynein and subsequent intracellular trafficking in a retrograde direction along microtubules explain the intracellular translocation of the Ad capsid to the microtubule organizing center, the final steps in trafficking of the Ad genome may require further motile forces and/or regulatory control. The recent observation that Ad capsids are capable of a highly stable interaction with the microtubule organizing

center in enucleated cells suggests that the interaction of Ad with the cytoplasmic dynein might have to be terminated prior to the localization of the capsid at the nuclear envelope (4). Alternatively, the eventual localization of the capsid to the nucleus may reflect the net result of the competing affinities of Ad for MAP-containing microtubules, versus the documented affinity of Ad for the nuclear envelope (10, 19, 66, 79). Further studies will be required to define the molecular events that bridge the gap between microtubule-dependent motility and nuclear envelope binding.

ACKNOWLEDGMENTS

We thank Richard B. Vallee, Columbia University College of Physicians and Surgeons, for helpful discussions and N. Mohamed for help in preparing the manuscript.

These studies were supported in part by NIH grant P01 HL51746, the Will Rogers Memorial Fund, and GenVec, Inc. K.K.P. was supported in part by the Jeffress Memorial Trust.

REFERENCES

1. **Alonso, C., J. Miskin, B. Hernaez, P. Fernandez-Zapatero, L. Soto, C. Canto, I. Rodriguez-Crespo, L. Dixon, and J. M. Escribano.** 2001. African swine fever virus protein p54 interacts with the microtubular motor complex through direct binding to light-chain dynein. J. Virol. **75:**9819–9827.
2. **Acsadi, G., R. A. Anguelov, H. Yang, G. Toth, R. Thomas, A. Jani, Y. Wang, E. Ianakova, S. Mohammad, R. A. Lewis, and M. E Shy.** 2002. Increased survival and function of SOD1 mice after glial cell-derived neurotrophic factor gene therapy. Hum. Gene Ther. **13:**1047–1059.
3. **Bai, M., B. Harfe, and P. Freimuth.** 1993. Mutations that alter an Arg-Gly-Asp (RGD) sequence in the adenovirus type 2 penton base protein abolish its cell-rounding activity and delay virus reproduction in flat cells. J. Virol. **67:**5198–5205.
4. **Bailey, C. J., R. G. Crystal, and P. L. Leopold.** 2003. Association of adenovirus with the microtubule organizing center. J. Virol. **77:**13275–13287.
5. **Baumgartner, B. J., and H. D Shine.** 1998. Neuroprotection of spinal motoneurons following targeted transduction with an adenoviral vector carrying the gene for glial cell line-derived neurotrophic factor. Exp Neurol. **153:**102–112.
6. **Bergelson, J. M., J. A. Cunningham, G. Droguett, E. A. Kurt-Jones, A. Krithivas, J. S. Hong, M. S. Horwitz, R. L. Crowell, and R. W. Finberg.** 1997. Isolation of a common receptor for Coxsackie B viruses and adenoviruses 2 and 5. Science **275:**1320–1323.
7. **Brady, S. T., K. K. Pfister, and G. S. Bloom.** 1990. A monoclonal antibody against kinesin inhibits both anterograde and retrograde fast axonal transport in squid axoplasm. Proc. Natl. Acad. Sci. USA **87:**1061–1065.
8. **Brady, S. T., R. J. Lasek, and R. D. Allen.** Video microscopy of fast axonal transport in extruded axoplasm: a new model for study of molecular mechanisms. Cell Motil. **5:**81–101.
9. **Chardonnet, Y., and S. Dales.** 1972. Early events in the interaction of adenoviruses with HeLa cells. 3. Relationship between an ATPase activity in nuclear envelopes and transfer of core material: a hypothesis. Virology **48:**342–359.
10. **Dales, S., and Y. Chardonnet.** 1973. Early events in the interaction of adenoviruses with HeLa cells. IV. Association with microtubules and the nuclear pore complex during vectorial movement of the inoculum. Virology **56:**465–483.
11. **Dales, S.** 1975. Involvement of the microtubule in replication cycles of animal viruses. Ann. N. Y. Acad. Sci. **253:**440–444.
12. **Davison, E., R. M. Diaz, I. R. Hart, G. Santis, and J. F. Marshall.** 1997. Integrin $\alpha5\beta1$-mediated adenovirus infection is enhanced by the integrin-activating antibody TS2/16. J. Virol. **71:**6204–6207.
13. **Dohner, K., A. Wolfstein, U. Prank, C. Echeverri, D. Dujardin, R. Vallee, and B. Sodeik.** 2002. Function of dynein and dynactin in herpes simplex virus capsid transport. Mol. Biol. Cell **13:**2795–2809.
14. **Everitt, E., H. Ekstrand, B. Boberg, and B. Hartley-Asp.** 1990. Estramustine phosphate reversibly inhibits an early stage during adenovirus replication. Arch. Virol. **111:**15–28.
15. **FitzGerald, D. J., R. Padmanabhan, I. Pastan, and M. C. Willingham.** 1983. Adenovirus-induced release of epidermal growth factor and pseudomonas toxin into the cytosol of KB cells during receptor-mediated endocytosis. Cell **32:**607–617.
16. **Garcia-Mata, R., Z. Bebok, E. J. Sorscher, and E. S. Sztul.** 1999. Characterization and dynamics of aggresome formation by a cytosolic GFP-chimera. J. Cell Biol. **146:**1239–1254.
17. **Ghadge, G. D., R. P Roos, U. J. Kang, R. Wollmann, P. S. Fishman, A. M. Kalynych, E. Barr, and J. M. Leiden.** 1995. CNS gene delivery by retrograde transport of recombinant replication-defective adenoviruses. Gene Ther. **2:**132–137.
18. **Gill, S. R., T. A. Schroer, I. Szilak, E. R. Steuer, M. P. Sheetz, and D. W. Cleveland.** 1991. Dynactin, a conserved, ubiquitously expressed component of an activator of vesicle motility mediated by cytoplasmic dynein. J. Cell Biol. **115:**1639–1650.
19. **Greber, U. F., M. Suomalainen, R. P. Stidwill, K. Boucke, M. W. Ebersold, and A. Helenius.** 1997. The role of the nuclear pore complex in adenovirus DNA entry. EMBO J. **16:**5998–6007.
20. **Greber, U. F., P. Webster, J. Weber, and A. Helenius.** 1996. The role of the adenovirus protease on virus entry into cells. EMBO J. **15:**1766–1777.
21. **Haase G, B. Pettmann, E. Vigne, L. Castelnau-Ptakhine, H. Schmalbruch, and A. Kahn.** 1998. Adenovirus-mediated transfer of the neurotrophin-3 gene into skeletal muscle of pmn mice: therapeutic effects and mechanisms of action. J. Neurol. Sci. **160**(Suppl. 1)**:**S97–S105.
22. **Hermens, W. T., and J. Verhaagen.** 1997. Adenoviral vector-mediated gene expression in the nervous system of immunocompetent Wistar and T cell-deficient nude rats: preferential survival of transduced astroglial cells in nude rats. Hum. Gene Ther. **8:**1049–1063.
23. **Hersh, J., R. G. Crystal, and B. Bewig.** 1995. Modulation of gene expression after replication-deficient, recombinant adenovirus-mediated gene transfer by the product of a second adenovirus vector. Gene Ther. **2:**124–131.
24. **Huang, S., T. Kamata, Y. Takada, Z. M. Ruggeri, and G. R Nemerow.** 1996. Adenovirus interaction with distinct integrins mediates separate events in cell entry and gene delivery to hematopoietic cells. J. Virol. **70:**4502–4508.
25. **Jacob, Y., H. Badrane, P. E. Ceccaldi, and N. Tordo.** 2000. Cytoplasmic dynein LC8 interacts with lyssavirus phosphoprotein. J. Virol. **74:**10217–10222.
26. **Johnston, J. A., M. E. Illing, and R. R. Kopito.** 2002. Cytoplasmic dynein/dynactin mediates the assembly of aggresomes. Cell Motil. Cytoskelet. **53:**26–38.
27. **Kalicharran, K., and S. Dales.** 1995. Involvement of microtubules and the microtubule-associated protein tau in trafficking of JHM virus and components within neurons. Adv. Exp. Med. Biol. **380:**57–61.
28. **King, S. M., E. Barbarese, J. F. Dillman III, R. S. Patel-King, J. H. Carson, and K. K. Pfister.** 1996. Brain cytoplasmic and flagellar outer arm dyneins share a highly conserved Mr 8,000 light chain. J. Biol. Chem. **271:**19358–19366.
29. **Kinoshita, N., T. Mizuno, and Y. Yoshihara.** 2002. Adenovirus-mediated WGA gene delivery for transsynaptic labeling of mouse olfactory pathways. Chem. Senses **27:**215–223.
30. **Kuo, H., D. K. Ingram, R. G. Crystal, and A. Mastrangeli.** 1995. Retrograde transfer of replication deficient recombinant adenovirus vector in the central nervous system for tracing studies. Brain Res. **705:**31–38.
31. **Leopold, P. L., B. Ferris, I. Grinberg, S. Worgall, N. R. Hackett, and R. G. Crystal.** 1998. Fluorescent virions: dynamic tracking of the pathway of adenoviral gene transfer vectors in living cells. Hum. Gene Ther. **9:**367–378.
32. **Leopold, P. L., G. Kreitzer, N. Miyazawa, S. Rempel, K. K. Pfister, E. Rodriguez-Boulan, and R. G. Crystal.** 2000. Dynein- and microtubule-mediated translocation of adenovirus serotype 5 occurs after endosomal lysis. Hum. Gene Ther. **11:**151–165.
33. **Luftig, R. B., and R. R. Weihing.** 1975. Adenovirus binds to rat brain microtubules in vitro. J. Virol. **16:**696–706.
34. **Luftig, R. B.** 1982. Does the cytoskeleton play a significant role in animal virus replication? J. Theor. Biol. **99:**173–191.
35. **Lukashok, S. A., L. Tarassishin, Y. Li, and M. S. Horwitz.** 2000. An adenovirus inhibitor of tumor necrosis factor alpha-induced apoptosis complexes with dynein and a small GTPase. J. Virol. **74:**4705–4709.
36. **Mabit, H., M. Y. Nakano, U. Prank, B. Saam, K. Dohner, B. Sodeik, and U. F Greber.** 2002. Intact microtubules support adenovirus and herpes simplex virus infections. J. Virol. **76:**9962–9971.
37. **Maccioni, R. B., and V. Cambiazo.** 1995. Role of microtubule-associated proteins in the control of microtubule assembly. Physiol. Rev. **75:**835–864.
38. **Martinez-Moreno, M., I. Navarro-Lerida, F. Roncal, J. P. Albar, C. Alonso, F. Gavilanes, and I. Rodriguez-Crespo.** 2003. Recognition of novel viral sequences that associate with the dynein light chain LC8 identified through a pepscan technique. FEBS Lett. **544:**262–267.
39. **Martinov, V. N., I. Sefland, S. I. Walaas, T. Lomo, A. Nja, and F. Hoover.** 2002. Targeting functional subtypes of spinal motoneurons and skeletal muscle fibers in vivo by intramuscular injection of adenoviral and adeno-associated viral vectors. Anat. Embryol. **205:**215–221.
40. **McDonald D, M. A. Vodicka, G. Lucero, T. M. Svitkina, G. G. Borisy, M. Emerman, and T. J. Hope.** 2002. Visualization of the intracellular behavior of HIV in living cells. J. Cell Biol. **159:**441–452.
41. **Miles, B. D., R. B. Luftig, J. A. Weatherbee, R. R. Weihing, and J. Weber.** 1980. Quantitation of the interaction between adenovirus types 2 and 5 and microtubules inside infected cells. Virology **105:**265–269.
42. **Millecamps, S., D. Nicolle, I. Ceballos-Picot, J. Mallet, and M. Barkats.** 2001. Synaptic sprouting increases the uptake capacities of motoneurons in amyotrophic lateral sclerosis mice. Proc. Natl. Acad. Sci. USA **98:**7582–7587.
43. **Millecamps, S., J. Mallet, and M. Barkats.** 2002. Adenoviral retrograde gene

transfer in motoneurons is greatly enhanced by prior intramuscular inoculation with botulinum toxin. Hum. Gene Ther. **13:**225–232.
44. **Mittereder, N., K. L. March, and B. C. Trapnell.** 1996. Evaluation of the concentration and bioactivity of adenovirus vectors for gene therapy. J. Virol. **70:**7498–7509.
45. **Miyazawa, N., P. L. Leopold, N. R. Hackett, B. Ferris, S. Worgall, E. Falck-Pedersen, and R. G. Crystal.** 1999. Fiber swap between adenovirus subgroups B and C alters intracellular trafficking of adenovirus gene transfer vectors. J. Virol. **73:**6056–6065.
46. **Murakami, T., I. Nagano, T. Hayashi, Y. Manabe, M. Shoji, Y. Setoguchi, and K. Abe.** 2001. Impaired retrograde axonal transport of adenovirus-mediated E. coli LacZ gene in the mice carrying mutant SOD1 gene. Neurosci. Lett. **308:**149–152.
47. **Paschal, B. M., E. L. Holzbaur, K. K. Pfister, S. Clark, D. I. Meyer, and R. B. Vallee.** 1993. Characterization of a 50-kDa polypeptide in cytoplasmic dynein preparations reveals a complex with p150GLUED and a novel actin. J. Biol. Chem. **268:**15318–15323.
48. **Paschal, B. M., H. S. Shpetner, and R. B. Vallee.** 1987. MAP 1C is a microtubule-activated ATPase which translocates microtubules in vitro and has dynein-like properties. J. Cell Biol. **105:**1273–1282.
49. **Pasick, J. M., K. Kalicharran, and S. Dales.** 1994. Distribution and trafficking of JHM coronavirus structural proteins and virions in primary neurons and the OBL-21 neuronal cell line. J. Virol. **68:**2915–2928.
50. **Peltekian, E., Garcia, L., Danos, O.** 2002. Neurotropism and retrograde axonal transport of a canine adenoviral vector: a tool for targeting key structures undergoing neurodegenerative processes. Mol. Ther. **5:**25–32.
51. **Petit, C., M. L. Giron, J. Tobaly-Tapiero, P. Bittoun, E. Real, Y. Jacob, N. Tordo, H. De The, and A. Saib.** 2003. Targeting of incoming retroviral Gag to the centrosome involves a direct interaction with the dynein light chain 8. J. Cell Sci. **116:**3433–3442.
52. **Raux, H., A. Flamand, and D. Blondel.** 2000. Interaction of the rabies virus P protein with the LC8 dynein light chain. J. Virol. **74:**10212–10216.
53. **Ridoux, V., J. J. Robert, X. Zhang, M. Perricaudet, J. Mallet, and G. Le Gal La Salle.** 1994. Adenoviral vectors as functional retrograde neuronal tracers. Brain Res. **648:**171–175.
54. **Rosenfeld, M. A., W. Siegfried, K. Yoshimura, K. Yoneyama, M. Fukayama, L. E. Stier, P. K. Paakko, P. Gilardi, L. D. Stratford-Perricaudet, M. Perricaudet, et al.** 1991. Adenovirus-mediated transfer of a recombinant alpha 1-antitrypsin gene to the lung epithelium in vivo. Science **252:**431–434.
55. **Schroer, T. A., and M. P. Sheetz.** 1991. Two activators of microtubule-based vesicle transport. J. Cell Biol. **115:**1309–1318.
56. **Shpetner, H. S., B. M. Paschal, and R. B. Vallee.** 1988. Characterization of the microtubule-activated ATPase of brain cytoplasmic dynein (MAP 1C). J. Cell Biol. **107:**1001–1009.
57. **Soudais, C., C. Laplace-Builhe, K. Kissa, and E. J. Kremer.** 2001. Preferential transduction of neurons by canine adenovirus vectors and their efficient retrograde transport in vivo. FASEB J. **15:**2283–2285.
58. **Suikkanen, S., K. Saajarvi, J. Hirsimaki, O. Valilehto, H. Reunanen, M. Vihinen-Ranta, and M. Vuento.** 2002. Role of recycling endosomes and lysosomes in dynein-dependent entry of canine parvovirus. J. Virol. **76:**4401–4411.
59. **Suikkanen, S., T. Aaltonen, M. Nevalainen, O. Valilehto, L. Lindholm, M. Vuento, and M. Vihinen-Ranta.** 2003. Exploitation of microtubule cytoskeleton and dynein during parvoviral traffic toward the nucleus. J. Virol. **77:**10270–10279.
60. **Suomalainen, M., M. Y. Nakano, S. Keller, K. Boucke, R. P. Stidwill, and U. F. Greber.** 1999. Microtubule-dependent plus- and minus end-directed motilities are competing processes for nuclear targeting of adenovirus. J. Cell Biol. **144:**657–672.
61. **Suomalainen, M., M. Y. Nakano, K. Boucke, S. Keller, and U. F. Greber.** 2001. Adenovirus-activated PKA and p38/MAPK pathways boost microtubule-mediated nuclear targeting of virus. EMBO J. **20:**1310–1319.
62. **Svensson, U., and R. Persson.** 1984. Entry of adenovirus 2 into HeLa cells. J. Virol. **51:**687–694.
63. **Takakuwa, H., F. Goshima, T. Koshizuka, T. Murata, T. Daikoku, and Y. Nishiyama.** 2001. Herpes simplex virus encodes a virion-associated protein which promotes long cellular processes in over-expressing cells. Genes Cells **6:**955–966.
64. **Terashima, T., A. Miwa, Y. Kanegae, I. Saito, H. Okado.** 1997. Retrograde and anterograde labeling of cerebellar afferent projection by the injection of recombinant adenoviral vectors into the mouse cerebellar cortex. Anat. Embryol. **196:**363–382.
65. **Tomko, R. P., R. Xu, and L. Philipson.** 1997. HCAR and MCAR: the human and mouse cellular receptors for subgroup C adenoviruses and group B coxsackieviruses. Proc. Natl. Acad. Sci. USA **94:**3352–3356.
66. **Trotman, L. C., N. Mosberger, M. Fornerod, R. P. Stidwill, and U. F. Greber.** 2001. Import of adenovirus DNA involves the nuclear pore complex receptor CAN/Nup214 and histone H1. Nat. Cell Biol. **3:**1092–1100.
67. **Turner, D. E., A. J. Noordmans, E. L. Feldman, and N. M. Boulis.** 2001. Remote adenoviral gene delivery to the spinal cord: contralateral delivery and reinjection. Neurosurgery **48:**1309–1316.
68. **Vale, R. D., T. S. Reese, and M. P Sheetz.** 1985. Identification of a novel force-generating protein, kinesin, involved in microtubule-based motility. Cell **42:**39–50.
69. **Valentine, R. C., and H. G Pereira.** 1965. Antigens and structure of the adenovirus. J. Mol. Biol. **13:**13–20.
70. **Vallee, R. B.** 1982. A taxol-dependent procedure for the isolation of microtubules and microtubule-associated proteins (MAPs). J. Cell Biol. **92:**435–442.
71. **Vasquez, E. C., R. F. Johnson, T. G. Beltz, R. E. Haskell, B. L. Davidson, and A. K. Johnson.** 1998. Replication-deficient adenovirus vector transfer of gfp reporter gene into supraoptic nucleus and subfornical organ neurons. Exp Neurol. **154:**353–365.
72. **Vincent, T., B. G. Harvey, S. M. Hogan, C. J. Bailey, R. G. Crystal, and P. L. Leopold.** 2001. Rapid assessment of adenovirus serum neutralizing antibody titer based on quantitative, morphometric evaluation of capsid binding and intracellular trafficking: population analysis of adenovirus capsid association with cells is predictive of adenovirus infectivity. J. Virol. **75:**1516–1521.
73. **Wagner, M. C., K. K. Pfister, G. S. Bloom, and S. T Brady.** 1989. Copurification of kinesin polypeptides with microtubule-stimulated Mg-ATPase activity and kinetic analysis of enzymatic properties. Cell Motil. Cytoskelet. **12:**195–215.
74. **Wang, K., S. Huang, A. Kapoor-Munshi, and G. Nemerow.** 1998. Adenovirus internalization and infection require dynamin. J. Virol. **72:**3455–3458.
75. **Warita, H., K. Abe, Y. Setoguchi, and Y. Itoyama.** 1998. Expression of adenovirus-mediated *E. coli* lacZ gene in skeletal muscles and spinal motor neurons of transgenic mice with a mutant superoxide dismutase gene. Neurosci. Lett. **246:**153–156.
76. **Weatherbee, J. A., R. B. Luftig, and R. R. Weihing.** 1977. Binding of adenovirus to microtubules. II. Depletion of high-molecular-weight microtubule-associated protein content reduces specificity of in vitro binding. J. Virol. **21:**732–742.
77. **Wickham, T. J., P. Mathias, D. A. Cheresh, and G. R. Nemerow.** 1993. Integrins alpha v beta 3 and alpha v beta 5 promote adenovirus internalization but not virus attachment. Cell **73:**309–319.
78. **Wickham, T. J., E. J. Filardo, D. A. Cheresh, G. R Nemerow.** 1994. Integrin alpha v beta 5 selectively promotes adenovirus mediated cell membrane permeabilization. J. Cell Biol. **127:**257–264.
79. **Wisnivesky, J. P., P. L. Leopold, R. G. Crystal.** 1999. Specific binding of the adenovirus capsid to the nuclear envelope. Hum. Gene Ther. **10:**2187–2195.
80. **Yamashita, S., S. Mita, T. Arima, Y. Maeda, E. Kimura, Y. Nishida, T. Murakami, H. Okado, and M. Uchino.** 2001. Bcl-2 expression by retrograde transport of adenoviral vectors with Cre-loxP recombination system in motor neurons of mutant SOD1 transgenic mice. Gene Ther. **8:**977–986.
81. **Yamashita, S., S. Mita, S. Kato, H. Okado, E. Ohama, and M. Uchino.** 2002. Effect on motor neuron survival in mutant SOD1 (G93A) transgenic mice by Bcl-2 expression using retrograde axonal transport of adenoviral vectors. Neurosci. Lett. **328:**289–293.
82. **Ye, G. J., K. T. Vaughan, R. B. Vallee, and B. Roizman.** 2000. The herpes simplex virus 1 U_L34 protein interacts with a cytoplasmic dynein intermediate chain and targets nuclear membrane. J. Virol. **74:**1355–1363.
83. **Ye, G. J., and B. Roizman.** 2000. The essential protein encoded by the UL31 gene of herpes simplex virus 1 depends for its stability on the presence of UL34 protein. Proc. Natl. Acad. Sci. USA **97:**11002–11007.